BMC Veterinary Research

RESEARCH

Open Access

Genomic analyses in Cavalier King Charles spaniels identify loci associated with clinical signs of Chiari-like malformation and Syringomyelia

Courtney R. Sparks[1], Jonah N. Cullen[2], Michael W. Vandewege[1], Meghan Leber[1], Katie M. Minor[2], Steven G. Friedenberg[2] and Natasha J. Olby[1,3*]

Abstract

Background Chiari-like malformations (CM) and syringomyelia (SM) are common in Cavalier King Charles spaniels (CKCS) leading to variable manifestations of pain and scratch. Inheritance studies suggest a polygenic mode of inheritance and association studies have identified loci associated with the presence of SM on MRI. Given the poor correlation of clinical signs of CMSM with MRI findings, we hypothesized that an association study with clinical signs as the phenotype could reveal new loci of interest. The objectives of this study were to perform genome-wide association studies on CKCS using SM and clinical sign phenotypes of pain and scratch and to use whole genome sequencing (WGS) to identify variants in regions of interest. We collected DNA on 174 CKCS. Owners completed questionnaires to establish the clinical pain and scratch phenotype and magnetic resonance imaging (MRI) was used to identify CM and SM (linear T2 hyperintensity greater than 2 mm in height) in all dogs. Dogs were genotyped using the Axiom K9 HD (710,000 snps) array. GWAS analyses were performed using GEMMA and categorical and quantitative approaches were used to define clinical phenotypes. Whole genome sequencing (WGS) was performed on an Illumina HiSeq 4000 high-throughput sequencing system.

Results There were no regions associated with SM presence. The presence of signs of pain and scratch was associated with a region on *Canis familiaris* autosome (CFA) 26 downstream of *ZWINT*, previously associated with skull changes in CKCS with SM, although genome-wide significance was not reached. Loci were also associated with quantitative pain and scratch scores on CFA 13, 2 and 38. There were 66 variants that segregated with phenotype including 2 missense variants that were predicted to have moderate effects on *ZWINT* function.

Conclusions The identification of a locus on CFA26 using the clinical phenotype of pain and scratch that coincided with a locus identified in a morphological study provides strong support for this as a region of interest.

Keywords Dog, Neuropathic pain, Genome-Wide association study, Neuropathic itch, Complex trait mapping

*Correspondence:
Natasha J. Olby
njolby@ncsu.edu
[1]Department of Clinical Sciences, College of Veterinary Medicine, North Carolina State University, Raleigh, NC, USA
[2]Department of Veterinary Clinical Sciences, University of Minnesota, Saint Paul, MN 55108, USA
[3]Comparative Medicine Institute, North Carolina State University, Raleigh, NC, USA

Background

Cavalier King Charles spaniels (CKCS) commonly suffer from Chiari-like Malformation and Syringomyelia (CMSM) that together can cause neuropathic pain and scratch [1–7]. Chiari-like malformation, considered ubiquitous within the breed, is a result of abnormal skull development that leads to overcrowding of the cerebellum and craniocervical junction(8). As a result of these conformational changes, it is hypothesized that alterations in CSF dynamics lead to the development of SM, fluid filled cavities within the spinal cord parenchyma, in approximately 70% of CKCS [8–13]. The clinical syndromes that result are complex with a syndrome in which pain predominates manifesting in dogs with CM alone, and a syndrome in which phantom scratch predominates in dogs with CM and SM [14]. There is considerable overlap between these syndromes, and simple presence or absence of CM and SM on MRI shows variable correlation with clinical signs. (2,8) Understanding of the pathogenesis of the clinical signs is evolving but centers on the impact of these morphological changes on sensory processing at various levels within the CNS (1).

The inheritance of CMSM has been studied in CKCS and has been shown to be complex [15–17]. The heritability of SM has been reported as moderate and breeding guidelines have been shown to reduce prevalence of CMSM within the breed [15, 18–20]. Canine genome-wide association studies (GWAS) have been an extremely successful tool for identifying simple, highly penetrant traits [21] and have been used to investigate complex traits [22]. Previous work, using GWAS methods, identified single nucleotide polymorphisms (SNPs) on *Canis familiaris* autosomes (CFA) 15, 22, and 26 that were associated with skull measurements that, in turn, are correlated to SM [23]. Similarly, SNPs were identified on CFA 2, 9, 12, 14, and 24 that were associated with skull measurements and CM in another breed commonly affected by CMSM, the Griffon Bruxellois [24]. These studies highlight the feasibility of GWAS to identify candidate loci in dogs with CMSM.

Table 1 Cohort characteristics of dogs with and without SM

	SM (*n* = 95)	No SM (*n* = 74)	Unknown (*n* = 5)
Sex (F, M)	62, 33	38, 36	1, 4
Age (years) (median, range)	3.35, 0.31–11.84	2.89, 1.06–8.92	2.72, 1.61–7.28
Showing clinical signs (n, %)	66, 70%	23, 31%	1, 20%
No clinical signs (n, %)	23, 24%	43, 58%	4, 80%
Unknown affected status (n, %)	6, 6%	8, 11%	0, 0%
TSS (median, range)[a]	6, 0–14.5	1.5, 0-15.5	6, 0–12
TPS (median, range)[a]	2, 0–18	0, 0–16	5, 0–10

[a] TSS and TPS were analyzed from 127 dogs

Within dog breeds, genetic diversity is greatly reduced due to selective breeding for breed-specific traits (i.e. coat color, body size). Additionally, the prevalence of CMSM in CKCS is high with an estimated 99% of CKCS affected by CM [5], and of those with CM an estimated 70% [8] also have SM. Because of this, it is possible that genetic variants may be fixed within the breed, making case-control GWAS approaches challenging. Another challenge in studying CMSM in CKCS stems from the fact that there is often incongruity between clinical signs and MRI findings. Numerous studies have reported a high incidence of clinically normal dogs with SM as well as those with classical clinical signs and no SM [2, 5, 8, 25–27]. To date, genetic approaches for studying CMSM in dogs have used MRI parameters as the phenotype, but the presence and severity of clinical signs have not been used to define phenotypes thus far. Given the lack of correlation between clinical signs and imaging findings, we were interested in mapping the clinical phenotype as well as the presence of SM in CKCS. The purpose of the current study was to use GWAS to identify genomic regions that are associated with clinical signs of pain and scratch as well as the presence of SM in CKCS.

Results

A total of 175 CKCS were entered into the study with MRIs, DNA samples, and general health questionnaires completed. Cohort characteristics are summarized in Table 1; Fig. 1 details the characterizations of phenotype for all study patients. Images were of inadequate quality to determine the presence of SM in 5 (3%) dogs. In 14 (19%) dogs, comorbidities such as skin disease or missing data meant that clinical status could not be clearly determined. These dogs were still included in the overall analyses using clinical status (for dogs without MRI phenotype) or SM status (for dogs without clinical phenotype); however, the missing data were labeled as unknown for each respective GWAS. Owners of 127 dogs completed the Chiari-like Malformation Pain and Scratch tool (ChiMPS-T) (Supplemental data 1). This survey asks owners about the presence, frequency and severity of signs of pain and scratching and the responses are allocated scores [2]. Total scratch score (TSS) and total pain score (TPS) were generated accordingly.

DNA samples were collected and genotyped on 712,331 snps using the Axiom K9 HD array. Cluster analysis revealed one sample was improperly labeled and determined to be a different dog breed; this dog was removed from analysis leaving 174 samples analyzed. A sex check test revealed correct identification for all dogs. All 174 dogs were included for the first GWAS case-control approach for both SM and clinical sign phenotypes. A total of 4 GWAS were performed: 1 case-control study for the presence of SM (174 dogs), 1 case-control study

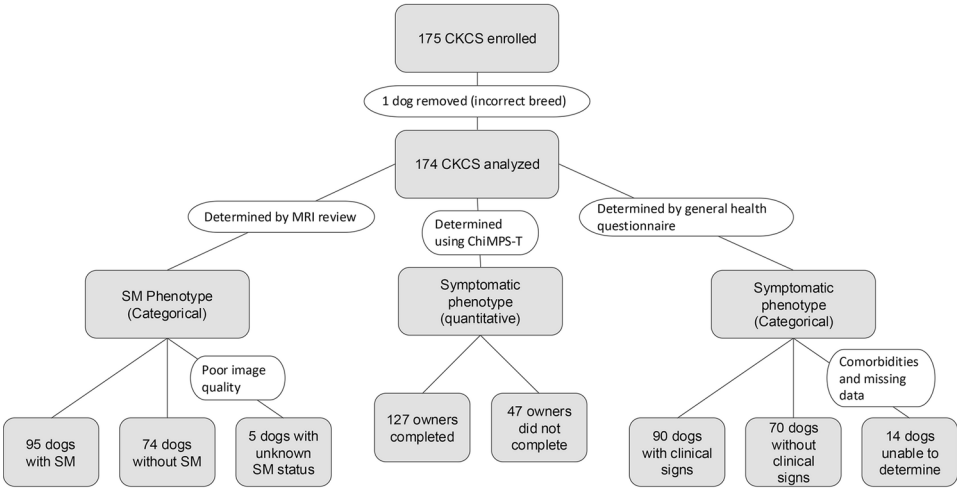

Fig. 1 Diagram of the methods and number of dogs analyzed for each categorical and quantitative phenotype

Table 2 Summary of GWAS parameters and data pruning for Syringomyelia and clinical sign phenotypes

	Syringomyelia Phenotype GWAS	**Clinical phenotype GWAS**	
Number of dogs analyzed	174	174	127
Sex (F, M)	101, 73	101, 73	72, 55
Approach	Case/Control	Case/Control	QTL (TSS, TPS, Combined TSS + TPS)
Number of Cases/Controls/Unknown	95/74/5	90/70/14	N/A
Variants Analyzed (n)	626,843	626,843	626,843
Dogs removed due to Missing Genotype Data (n)	0	0	0
Variant Removed due to Missing Genotype Data (n)	0	0	0
Total Genotyping Rate (%)	99.8%	99.8%	99.7%
Variants removed due to HWE exact test (n)	5075	2828	5984
Variants removed due to MAF < 0.01	280,993	280,993	276,805
Total Variants remaining for analysis (n)	**340,775**	**343,022**	**344,054**

for the presence of clinical signs (174 dogs), and 2 quantitative approaches (127 dogs) for clinical signs using TSS and TPS. A summary of GWAS parameters and pruning results for all analyses is shown in Table 2.

Genome-wide association study – case/control approaches

A GWAS using a univariate linear model with age as a covariate was applied to our characterizations of phenotype. Our first case/control approach compared dogs with and without SM and the results are shown in Fig. 2a. No locus was significantly associated with the SM phenotype (all $p > 1e\text{-}5$). Next, we evaluated the presence or absence of clinical signs, including pain and scratch, in all 174 dogs (Fig. 2b). This resulted in the identification of 9 SNPs on CFA 26 associated with the presence of clinical signs (all $p < 1e\text{-}5$)(Table 3). These SNPs replicated previous findings from a GWAS that used skull measurements associated with SM to identify a locus on CFA 26 from 32,735,128 to 32,738,238 bp. The region containing these SNPs is situated near the *ZWINT* gene (ZW_{10} Interacting Kinetochore Protein) and expression of this gene has been shown to increase with neuropathic pain [28–30]. This region is significantly associated with skull morphometry variables in CKCS that are predictive of SM [23], as demonstrated in previous work, as well as with the presence of clinical signs in our cohort of CKCS.

Genome-wide association study – quantitative approach

Next, GWAS analyses were performed using QTL approaches with quantification of clinical signs (TSS and TPS) and the results are shown in Fig. 3. The TSS phenotype mapped to regions on CFA 2 and 38 (Table 4) including 9 significantly associated SNPs ($p < 1e\text{-}5$). The peak SNPs on CFA 2 are in a location containing the *KIAA1217* (Sickle Tail Protein Homolog) gene, which is required for normal development of intervertebral discs (https://www.genecards.org/cgi-bin/carddisp.pl?gene=KIAA1217). The 2 loci on CFA 38 are located in intergenic regions near the *SUSD4* gene which encodes a transmembrane protein that is highly expressed in nervous tissue and is involved in the complement system (https://www.genecards.org/cgi-bin/carddisp.pl?gene=SUSD4).

When using TPS as an ordinal scale of pain, there was a group of 20 associated SNPs identified on CFA 13 (Fig. 2b; Table 4). These SNPs are located in a region containing the *KCTD8* (Potassium Channel Tetramerization Domain Containing 8) gene. This gene encodes a

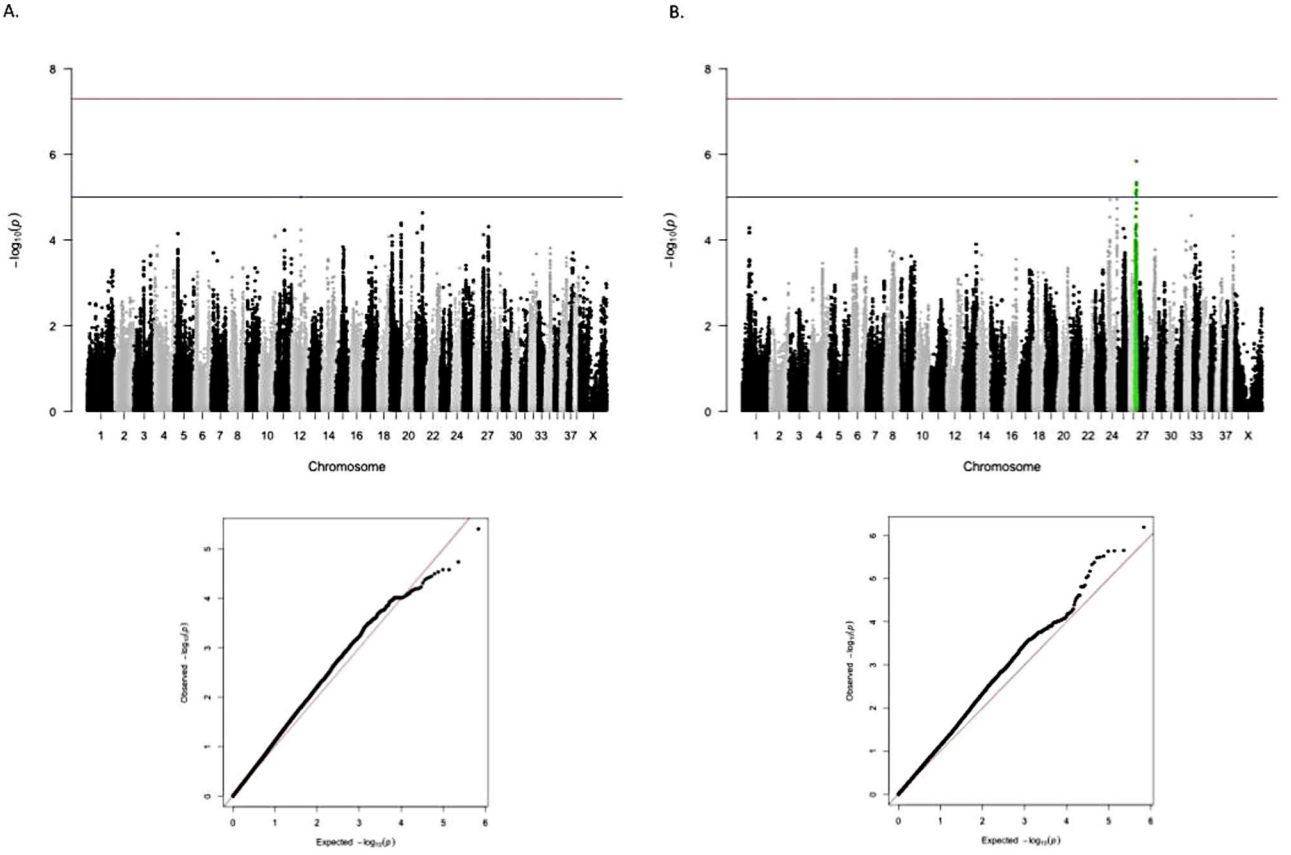

Fig. 2 Manhattan plots (top) and QQ plots (bottom) of loci identified using a univariate linear model case/control association study for the categorical phenotypes: (**a**) SM and (**b**) Clinically affected. A locus on CFA26 reached the threshold suggestive of significance with the presence of clinical signs (green). SM: syringomyelia. Black horizontal line: $p < 1 \times 10^{-5}$, suggestive of significance, red horizontal line: $p < 5 \times 10^{-8}$, reaching genome-wide significance

Table 3 Loci significantly associated with categorical phenotypes

Chromosome	SNP	Position	*P* value
Clinically Affected Case-Control GWAS			
26	AX-167,722,786	32,810,375	1.43e-06
26	AX-167,835,112	32,751,879	4.50e-06
26	AX-167,701,085	32,755,912	5.06e-06
26	AX-167,726,693	32,817,412	5.11e-06
26	AX-167,592,907	32,706,507	6.72e-06
26	AX-168,001,132	32,711,258	7.07e-06
26	AX-167,520,772	32,691,954	7.28e-06
26	AX-168,238,977	29,302,917	8.092e-06
26	AX-168,050,640	32,786,452	8.78e-06

potassium channel that is located on the auxiliary subunit of GABA-B receptors and may contribute to neuropathic pain signaling in dorsal horn neurons (https://www.genecards.org/cgi-bin/carddisp.pl?gene=KCTD8). Regions of LD were estimated (r^2) surrounding each peak SNP on CFA 2, 38, 13, and 26 and are summarized in Table 5.

Whole genome sequencing

Whole genome sequencing data from 21 CKCS and 501 control dogs of other breeds were used to investigate our regions of LD surrounding our peak SNPs on CFA 2, 38, 13, and 26. Of the 21 CKCS, 4 showed clinical signs with SM, 3 were normal, 2 showed no clinical signs with SM, and 12 had unknown phenotypes and were a part of a database that is shared with NCSU and the University of Minnesota. The 501 control breed dogs were also a part of the multi-institution database of WGS data that included dogs from breeds with specific cardiac or neurologic conditions distinct from CMSM. The breakdown of breeds is provided as supplementary data (Supplemental data 2). There were 148,558 variants (biallelic and multiallelic) for all 4 regions impacting a total of 19 genes. Detailed information on variants for each region of LD surrounding the lead SNPs are shown in Table 6. We were particularly interested in variants that were segregated with phenotype. Thus, we filtered the variants such that all 4 CKCS with clinical signs were homozygous for the variant and at least 80% of the 5 clinically normal CKCS had no variant. After filtering the data, 66

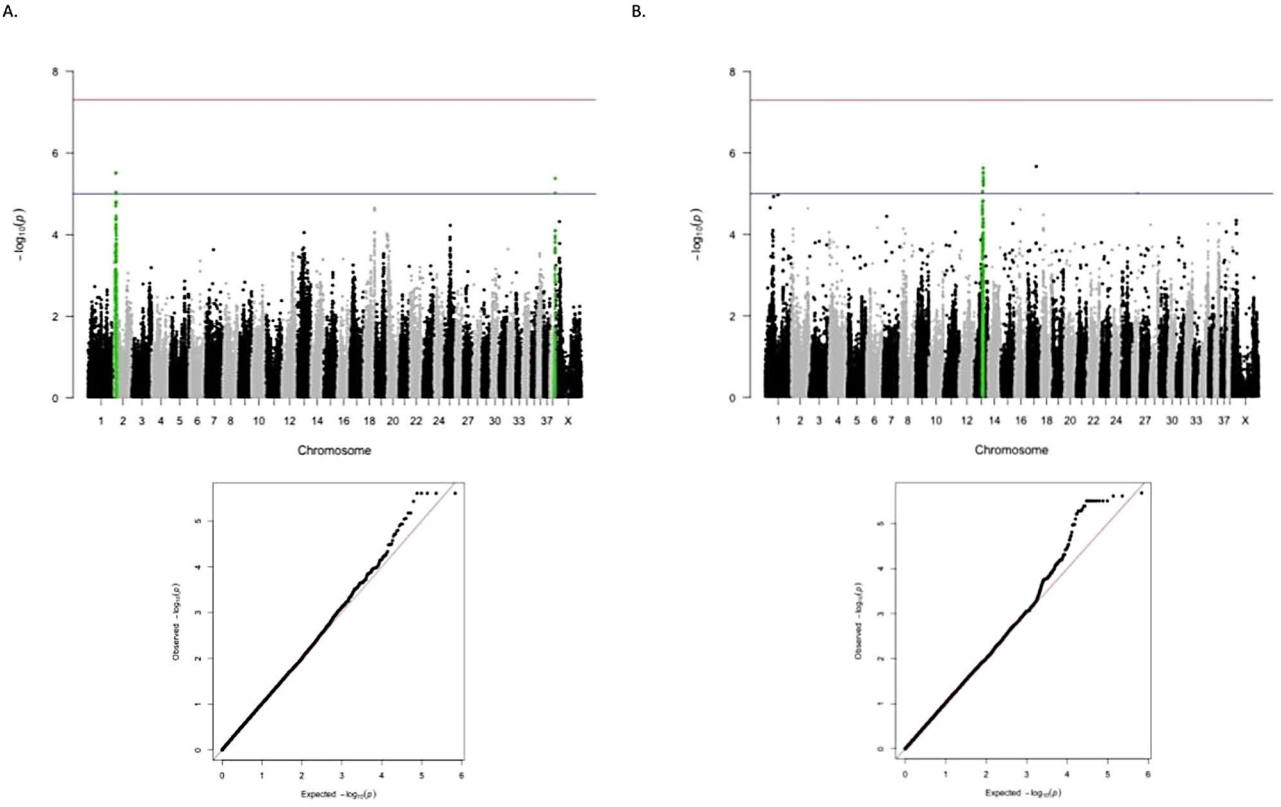

Fig. 3 Manhattan plots (top) and QQ plots (bottom) of loci identified using a univariate linear model quantitative trait analysis for the quantitative phenotypes: (**a**) TSS and (**b**) TPS. Two loci on CFA2 and CFA38 was significantly associated with TSS (green) and one locus on CFA13 was significantly associated with TPS (green). TSS: total scratch score; TPS: total pain score. Black horizontal line: $p < 1 \times 10^{-5}$, suggestive of significance, red horizontal line: $p < 5 \times 10^{-8}$, reaching genome-wide significance

Table 4 Loci significantly associated with TSS and TPS

CFA	SNP	Position	*P* value	CFA	SNP	Position	*P* value
TSS				TPS continued			
2	AX-167,822,102	9,009,354	3.103431e-06	13	AX-167,740,621	40,855,722	3.04e-06
2	AX-167,199,713	9,011,589	3.103431e-06	13	AX-167,201,105	40,882,198	3.04e-06
2	AX-167,994,378	9,049,119	3.103431e-06	13	AX-167,652,582	40,899,335	3.04e-06
2	AX-167,172,978	9,049,327	3.103431e-06	13	AX-167,179,400	40,915,607	3.04e-06
2	AX-168,057,275	9,143,798	3.103431e-06	13	AX-168,090,093	40,916,385	3.04e-06
38	AX-167,960,206	23,617,547	4.200984e-06	13	AX-167,158,069	40,926,093	3.04e-06
2	AX-167,643,321	9,121,165	9.197832e-06	13	AX-167,655,016	40,827,553	3.91e-06
2	AX-167,433,092	9,150,433	9.197832e-06	13	AX-168,018,250	40,923,743	4.55e-06
38	AX-167,862,318	23,620,455	9.635262e-06	13	AX-167,823,206	40,816,784	5.084e-06
TPS				13	AX-167,867,298	40,862,806	5.084e-06
17	AX-167,899,205	42,805,289	2.119375e-06	13	AX-167,595,827	40,907,266	5.084e-06
13	AX-168,167,845	40,834,152	2.342315e-06	13	AX-167,875,295	40,921,082	5.084e-06
13	AX-168,182,488	40,836,369	2.342315e-06	13	AX-167,335,747	40,903,390	5.77e-06
13	AX-167,891,564	40,844,273	3.043704e-06	13	AX-167,554,609	40,918,644	6.22e-06
13	AX-167,894,838	40,853,536	3.043704e-06	13	AX-168,089,890	37,027,653	8.78e-06
13	AX-167,202,221	40,854,605	3.043704e-06	26	AX-168,264,840	24,414,228	9.52e-06

variants remained. All of the variants are located on CFA 26 and impact the *ZWINT* gene. Of these variants, 61 are predicted to have modifying effects on gene function, 3 are predicted to have low impacts on gene function, and the remaining 2 are expected to have moderate effects on gene function. Detailed information on the variants predicted to have moderate effects on *ZWINT* function are displayed in Table 7. These 2 variants are situated

Table 5 Regions of LD surrounding each peak SNP. The genes closest to the significantly associated SNPs were KIAA1217, SUSD4, KCTD8; respectively (in bold)

Chromo-some	Peak SNP	Position (bp)	Region of Linkage Disequilibrium (LD) (bp range)	Genes located within the region of LD
2	AX-167,822,102	9,009,354	8,124,511–9,894,677	ARHGAP21, C2H10orf67, ENKUR, GPR158, **KIAA1217**, OTUD1, PRTFDC1, THNSL1
38	AX-167,960,206	23,617,547	23,331,252–23,823,235	CCDC185, CD1A6, CD1C, CD1D, DISP1, KIRREL1, LOC608848, LOC610726, **SUSD4**, TLR5
13	AX-168,167,845	40,834,152	39,859,426–41,228,753	GNPDA2, GRXCR1, GUF1, **KCTD8**, LOC102156956, LOC102157179, LOC482124, YIPF7
26	AX-167,722,786	32,810,375	32,110,995–32,857,256	ZWINT

Table 6 Summary of variants identified in specified regions of LD

Chromosome: region	Variants (*n*)	Variant effects (*n*)	Impact of Variant effects				Annotated Genes (*n*)
			High	Moderate	Low	Modifier	
2: 8,124,511–9,894,677	78,380	22	136	555	439	77,250	7
38: 23,331,252–23,823,235	51,667	27	96	553	547	50,471	6
13: 39,859,426–41,228,753	13,240	24	13	58	67	13,102	6
26: 32,110,995–32,857,256	5,271	14	2	9	13	5,247	1

Table 7 A summary of the 2 variants predicted to have a moderate impact on *ZWINT* gene function. The number and percentage of dogs that were homozygous wildtype, homozygous for the variant, and heterozygous are shown, differentiated by clinical status

		ZWINT	
Chromosome: Position		26: 32,434,594	26: 32,434,684
Homozygous wildtype	% Clinically Affected CKCS (*n* = 4)	0	0
	% Clinically normal CKCS (*n* = 5)	80	80
	% Unknown phenotype CKCS (*n* = 12)	16.7	16.7
	% Control Dogs (*n* = 501)	21.4	7.0
Homozygous Variant	% Clinically Affected CKCS (*n* = 4)	100	100
	% Clinically normal CKCS (*n* = 5)	20	20
	% Unknown phenotype CKCS (*n* = 12)	50	50
	% Control Dogs (*n* = 501)	39.2	67.4
Heterozygous Variant	% Clinically Affected CKCS (*n* = 4)	0	0
	% Clinically normal CKCS (*n* = 5)	0	0
	% Unknown phenotype CKCS (*n* = 12)	33.3	33.3
	% Control Dogs (*n* = 510)	39.4	25.6
Consequence of Variant		missense	missense
Reference: Alternate		G: A	G: A

at bp 32,434,594 and 32,434,684. One clinically normal CKCS (20%) was homozygous for both variants while the remainder of the clinically normal CKCS(80%) were wild type homozygous. Linkage disequilibrium between these two variants are the lead SNP (AX-167722786) is 0.7 (32434594) and 0.72 (32434684).

Structural variant detection and validation

We used the WGS data from eight CKCS dogs, each with distinct phenotypes: three normal, two with clinically silent SM, and three showing clinical signs with SM to explore the potential influence of structural variants (SV) on these phenotypes. One specific SV was a 2.5 kb tandem duplication located downstream of the ZWINT gene, situated within the linkage disequilibrium (LD) boundaries of AX-167,722,786 (chr26:32817412). This predicted SV was notably associated with the clinically affected phenotype. Specifically, the duplication was predicted absent in the three dogs showing clinical signs, and present in all dogs lacking clinical signs, while no other SVs showed a relationship with CM or pain and scratch. To validate our results, we performed DNA extraction from a sample of five CKCS dogs, consisting of three normal and two affected by SM, including one normal and one clinically affected dog from the original WGS dataset. Utilizing long-range PCR, we isolated and sequenced the annotated region along with an additional 1 kb of flanking sequence. This resulting fragment spanned chr26:32,509,985 – 32,514,838. However, the duplication identified by LUMPY was absent in the long-range sequences.

Discussion

Given the high prevalence and complex inheritance of CMSM in CKCS, simply eliminating dogs that produce CMSM from breeding programs will not necessarily eradicate the disease. Further, mass elimination of dogs from the breeding pool may increase the risk of other genetic disorders. In fact, selective breeding for specific coat colors in CKCS is believed to have contributed to the development of abnormal skull morphology [16]. Thus, the primary goal of this study was to identify genetic markers associated with the presence of SM and with clinical signs in CKCS. In particular, we were interested in loci associated with the clinical phenotype

rather than morphological features due to the reports of discrepancies between MRI findings of SM and the presence of clinical signs in dogs with CMSM [2, 5, 8, 25–27]. The perplexing nature of CMSM with regards to inconsistencies in structural changes versus clinical phenotype led to our hypothesis that there may be a genetic underlying cause that predisposes some CKCS to develop clinical signs while others remain clinically normal.

In this study, we prospectively recruited 175 CKCS with varying morphological and clinical phenotypes. In agreement with previous studies, we found disparities in clinical presentation and MRI findings in this cohort as 31% of dogs without SM were clinically affected and, conversely, 24% of dogs with SM were clinically normal. Given these differences, we first investigated whether genetic differences could be identified among dogs with and without SM using a straightforward case-control GWAS study. This analysis was of low yield resulting in no loci of interest. The age at time of MRI was highly variable in this study; thus, it is possible that morphologic evidence of disease was not yet present in some dogs. Also, we defined the presence of SM as any syrinx measuring ≥ 2 mm in height and, given the progressive nature of this disease, it is likely that dogs with canal dilation (measuring less than 2 mm) may develop SM in the future [4]. Previous studies have identified associations between the size and distribution of SM with clinical signs; therefore, a more detailed analysis may be necessary to account for syrinx characteristics. Nonetheless, these results combined with the overall lack of correlation between MRI findings and clinical signs provided further support for the use of clinical status to define phenotype in further genetic analyses.

Establishing the clinical phenotype in this condition is fraught with difficulty because of the need for observers to interpret behaviors shown by dogs as signs of pain. In addition, there are many comorbidities that can cause both pain and scratching. Medical records were used to identify any potential condition that could present as a phenocopy and these were excluded from clinical analyses, but reliance on the medical history alone could result in inaccuracies. Magnetic resonance images were available in all dogs allowing other spinal conditions to be ruled out as a source of pain. To investigate the significance of clinical phenotypes, we began with a simple categorical approach (clinical signs of pain and or scratch: yes or no) and we identified a locus that suggested significance on CFA26. These results corroborate the findings of previous work done by Ancot et al., whereby a locus on CFA26 was found to be significantly associated with skull measurements that reflect a reduced caudal fossa in CKCS [23]. This particular skull measurement was shown to be correlated with syrinx transverse diameter [23]. The agreement between our two studies that addressed the complex syndrome associated with CMSM using very different methods of establishing the phenotype lends further support to this being an important locus in CKCS.

The only coding gene in this region is *ZWINT*, a gene that encodes a protein that is involved in kinetochore function and chromosome segregation [31]. The *ZWINT* gene is highly expressed in the brain and dorsal horn laminae and is a known modulator of neurotransmitter release [28, 32]. A chronic neuropathic pain model has revealed ZWINT expression is increased with neuropathic pain in rodents [28–30]. In contrast to the present study, Ancot et al. failed to show an association between this region and pain in a cohort of 65 dogs [23]. The authors acknowledged that pain phenotyping was limited at the time of DNA sampling and dogs were only differentiated by the presence or absence of SM; therefore they did not account for the cases where MRI findings are inconsistent with clinical presentation [23]. In this study, we failed to detect an association between this region and SM; but, by using a larger cohort of dogs with detailed phenotypic definitions of clinical signs (regardless of SM diagnosis) we identified an association between this region and the presence of clinical signs. While WGS analysis did not reveal any high impact variants, we did identify two mutations that predicted a moderate effect on *ZWINT* function. These mutations were present in all of our clinically affected dogs while the majority of clinically normal dogs did not carry the mutations. Ten (83%) CKCS with unknown phenotypes had the mutations as well. Although these mutations seemed to segregate well with clinical sign presentation in CKCS, they were also highly prevalent in control breed dogs demonstrating that these are common canine variants. Finally, a structural variant, 2.5 kb tandem duplication, was identified downstream of the ZWINT gene and was clearly associated with the presence of clinical signs, but this was unfortunately a false positive, revealed by PacBio sequencing. Although disease-causing genetic variant discovery has largely focused on coding regions, it has become clear in recent years that the non-coding genome harbors an abundance of variants that contribute to genetic disease. In fact most GWAS studies in humans map to non-coding regions [33]. Unfortunately, non-coding variants are difficult to interpret and require additional analyses to effectively understand their role. A well understood role of a fraction of the non-coding genome is gene regulation. Future work may focus on gene expression differences between dogs with and without signs of pain and scratch through RNA sequencing. Further, additional lab techniques like assay for transposase-accessible chromatin with sequencing (ATACseq) and Chromatin immunoprecipitation sequencing (ChIP-seq)

can reveal epigenetic loci that could be relevant to this complex disease.

Our quantitative GWAS approaches investigated scratch and pain signs using ordinal scales, TSS and TPS. These analyses provided a way to capture the wide-ranging spectrum of clinical signs that are observed in CKCS with CMSM. There were multiple snps at the $P < 10^{-5}$ significance level on CFA 2, 13, and 38. Interestingly, the loci of interest were distinct when clinical signs were differentiated by scratch (CFA 2 and 38) or pain (CFA 13). To further support this concept, a retrospective study identified that scratching-related signs were associated with the size of SM; however, pain signs were present regardless of the presence or severity of SM [8]. In addition, another study hypothesized that large dorsolateral syrinxes cause damage to the dorsal horn such that lumbar scratching central pattern generators are disrupted causing a fictive type scratch [34]. Hence, it's plausible that scratching related signs in dogs with CMSM are as a result of physical damage to the dorsal horn whereas pain signs may involve a genetic component including altered pain processing.

The scratch phenotype, as quantified by TSS, mapped to 2 regions on CFA 2 and 38 that were closest to KIAA1217 and SUSD4, respectively. KIAA1217 gene encodes a sickle cell protein homolog that is predicted to play a role in skeletal system development [35] and SUSD4 is highly expressed in the nervous system and plays a role in the complement system. In contrast, when we investigated pain on a continuous scale using GWAS, we found a compelling locus on CFA13. The significantly associated snps were all situated in a region containing *KCTD8*. Importantly, *KCTD8* encodes a protein that has a tetramerization domain which binds to GABA-B receptors [36]. GABA-B receptors are inhibitory neurotransmitter receptors and their signaling is tightly regulated by KCTD domains [37, 38]. The distribution of expression of *KCTD8* in the rodent brain has been shown to be found in the medial habenula, brainstem nuclei, and the cerebellum [39]. Variations in expression of *KCTD8* are associated with brain size in adolescent human females [40] and there is some evidence it is associated with obesity in Labrador retrievers [41]. The role of *KCTD8* in dorsal horn interneurons is still largely unknown but due to its intimate connection and modulation of GABA receptors, it is an interesting candidate gene to consider with regards to pain in CKCS with CMSM. When analyzing WGS data, there were 33 mutations that were predicted to have moderate to high impact on *KCTD8* expression and thousands more that were modifiers. Unfortunately, the majority of these variants had a high degree of missing variant data for our CKCS of known phenotypes making it difficult to compare variant effects with clinical signs. Additional exploration of these variants in dogs with well-documented pain phenotypes is warranted.

Conclusion

The CMSM condition in dogs is complex and most likely polygenic. There are likely several genes that are involved in the clinical manifestation of CMSM in dogs. The replication of the locus in the region of *ZWINT* between a study using skull morphometry and our study using clinical phenotype adds to the evidence that this region is important in clinical CMSM in CKCS. More work is required to investigate the genomic regions of interest identified in this study. Sanger sequencing of these regions and snps in well phenotyped dogs would allow for additional insight into whether these regions segregate with clinical signs. This is particularly important for the *KCTD8* variants that were identified on WGS but had a high degree of missing variant call data. Finally, we used stringent criteria for analyzing variants from our WGS data in this study including mostly variants with high or moderate predictive impact. The CMSM condition in dogs is rarely fatal, and therefore it is possible that mutations causing modifications of gene function are also relevant. Detailed investigation of all mutations that are considered "modifiers" is warranted. If haplotype analyses and sanger sequencing results suggest genes or snps that are associated or are segregating with clinical signs; then, tagsnps could be used to efficiently genotype a large cohort of well-phenotyped CKCS in the regions of interest.

To summarize, we collected DNA, MRIs, and detailed information on clinical signs in a large cohort of CKCS. We found that by differentiating dogs on the basis of clinical signs, rather than the presence of SM, we were able to detect several regions of interest including snps that replicated previously published findings that used a morphological measure of phenotype rather than a functional one. We used categorical and continuous measures of clinical signs to classify phenotypes and found snps on CFA 2, 13, 26, and 38. Within these regions, we identified 2 moderate impact mutations affecting the *ZWINT* gene. Further work is warranted to determine the segregation of these regions and genes with disease in dogs with CMSM.

Methods

Dogs and sample collection

Clinically normal and affected CKCS were recruited through advertisements on North Carolina State's Veterinary Hospital (NC State VH) webpage, by referral from veterinary general practitioners and neurologists, and from dogs being seen through NC State VH. All dogs were privately owned as pets or breeding dogs. All owners reviewed an informed consent form, were given the

opportunity to ask questions and signed the form. All procedures were approved by NCSU's Institutional Animal Care and Use Committee (Protocol #15-003-O).

Study involvement required digital copies of MRIs of the cervical spine and brainstem at minimum, DNA sample (blood or saliva), and completion of a general health questionnaire by owners. The general health questionnaire included questions regarding the presence of clinical signs of CMSM as well as whether the dog suffered from comorbidities that could also cause pain and/or scratch. Additionally, a clinical metrology instrument (CMI) was used to quantify pain and scratch associated with CMSM (Supplemental data 1) [2]. Medical records were reviewed by the investigators and the dogs were examined by the investigators wherever possible, however, this was not a requirement of the study. Whole blood or saliva samples were collected on all dogs. Extraction of DNA was performed from whole blood using QIAamp DNA Blood Midi Kit (Qiagen; Valencia, CA), and from saliva using QIAamp DNA Mini Kit (Qiagen; Valencia, CA). A NanoDrop 2000 spectrophotometer (Thermo Scientific; Wilmington, DE) was used to measure DNA concentrations. Informed consent was read and approved by owners and all procedures were approved by NCSU's Institutional Animal Care and Use Committee (Protocol #15-003-O).

Phenotype determination: Syringomyelia

Magnetic resonance images were reviewed to ensure that there was no other possible cause of clinical signs. Horos Medical Imaging Software (Open Source Software, https://horosproject.org*)* and eUnity software (V ersion 6.3.0.1.4, Client Outlook Ink, Waterloo, Ontario) were used to evaluate images in Digital Imaging and Communication (DICOM) format. The presence of SM was determined using T2-sagittal images of the cervical spinal cord. Dogs with linear T2 hyperintense signals measuring more than 2 mm in height were determined to have SM. The SM phenotype was recorded as unknown for dogs with inadequate images or poor image quality; however, these dogs remained in the analysis because of the usefulness of their clinical phenotype information.

Presence and severity of clinical signs

Clinical status was assigned both categorically and quantitatively. The presence of clinical signs (categorical assessment) of CMSM was determined by collecting a detailed history, reviewing medical records, and by completion of a general health questionnaire that was required for involvement in the study. This information was used to identify dogs with a history of skin disease, ear disease or allergies that could cause scratching, or orthopedic, spinal or other neurologic disease that could cause pain. Dogs were categorized as having pain and or scratch if the owners reported signs occurring at minimum every week. The severity of clinical signs was determined using a disease-specific CMI that was developed and instituted partway through enrollment of the study, known as the Chiari-like malformation pain and scratch tool (ChiMPS-T) [2] (Supplemental data 1). This questionnaire captures the presence, frequency and severity of owner reported signs of scratch and pain. A small cohort of dogs had already had DNA and phenotypes collected prior to development of ChiMPS and so these were not included in the analyses performed using TSS and TPS scores (Fig. 1). Responses were developed into scores reflecting scratch and pain (total scratch score, TSS (range 0–16); total pain score, TPS (range 0–20)). Dogs with comorbidities that could cause pain or scratch were recorded as unknown for the clinically affected phenotype; they remained in the study for the SM phenotype analysis.

Genotyping and data analysis

A total of 175 dogs were genotyped using the Applied Biosystems Axiom K9 HD (710,000 snps) array (Thermo Fisher Scientific, Santa Clara, CA). Our goal was to genotype 192 dogs based on published power analyses of complex traits [21, 22] with a minimum of 70 dogs based on a prior GWAS study of Cavalier King Charles spaniels using skull morphometry [23].

The assays were performed by Thermo Fisher Scientific according to the manufacturer's instructions and files were returned as VCF, CEL, and ARR files to be viewed in Axiom Analysis Suite Software. Axiom Analysis Suite software was used to generate.PED and.MAP files combining the genotype data for both cohorts. The genotypes were pruned using PLINK (Version v1.90b6.9) whereby data were removed if minor allele frequency was less than 5%, snp genotyping rate was less than 90%, individual genotype data was less than 90%, and if markers failed the Hardy-Weinberg test at the $P=.005$ level. A sex check test was performed in PLINK as a quality control measure. Next, GEMMA (version 0.98) was used to fit a univariate linear model and perform case/control and quantitative trait association studies while accounting for population structure and stratification [41]. A centered relatedness matrix was generated (-gk 2), eigen decomposition was performed on the relatedness matrix (-eigen), and likelihood ratio tests were performed (-lm 2). Given the increased prevalence of SM and clinical signs with age [4, 29], we included age as a covariate for all analyses. Analyses were performed using SM (yes or no) and clinical signs (presence: yes or no; severity: TSS and TPS) phenotypes. Linkage disequilibrium (LD) for each lead SNP was calculated using r^2 decay to a value of 0.6.

Whole genome sequencing

Eight CKCS including 3 normal CKCS, 3 severely clinically affected with SM, and 2 clinically normal CKCS with SM were sequenced. Whole genome sequencing was performed at Genewiz LLC Next-Generation Sequencing Laboratory, using a 150 bp paired-end read configuration in a single lane of an Illumina HiSeq 4000 high-throughput sequencing system. Variant calling from WGS data was performed using a standardized bioinformatics pipeline for all samples as described previously [42]. Variants that segregated with clinical phenotype were identified and examined for potential impact on protein expression and function, and gene relevance.

Structural variant query and validation

We used LUMPY [43] to detect structural variants (SVs) in the 8 WGS samples above. Specifically, we used Smoove 0.2.8 (https://github.com/brentp/smoove) which integrates LUMPY best practices and other tools to detect SVs. Briefly, SVs were called independently in each sample, SVtools 0.5.1 [44] merged SV calls across samples, SVs were genotyped with SVtyper 0.7.1 [45] and annotated with depth of coverage using Duphold 0.2.1 [46]. SVs were filtered based on Duphold annotations. Deletions with DHFFC (fold change of the variant) < 0.7, duplications with DHFFC > 1.3 and inversions with DHFFC between 0.7 and 1.3 were retained, per the instructions' recommendation. SVs within linkage distances of notable snps (Table 5) were further investigated.

We developed primers flanking a predicted duplication using Primer3 and the CanFam3 assembly (Forward: 5'-AGGGTCCAGAAATATCCTGTCTTT-3'; Reverse: 5-TGACGGAGAAACTGT CCT CCT-3'). For the long range PCR, 49 µl mastermix (25 µl type of Platinum™ SuperFi™ PCR Master Mix, 8 µl nuclease-free water, 8 µl of 5 µM or each primer) was combined with 1 µl extracted DNA. Thermocycling conditions consisted of an initial denaturation step of 30 s at 98 C, then 45 cycles (10 s at 98 C, 10 s at 66 C, 3 min 45 s at 72 C) and a final extension step of 5 min at 72 C. PCR products were visualized on 1% TBE agarose gels. PCR products were purified using a commercial PCR purification kit (GeneJET PCR Purification kit, Thermo Fisher Scientific Inc.). PacBio library prep and sequencing were performed by Genewiz. Hifi reads were mapped to the reference genome using minimap2 [47] and SVs were called with PBSV.

Abbreviations

CFA	Canis familiaris autosome
CKCS	Cavalier King Charles Spaniel
CM	Chiari-like malformations
ChiMPS-T	Chiari-like Malformation Pain and Scratch tool
DICOM	Digital Imaging and Communication
GWAS	Genome-wide Association Study
LD	Linkage Disequilibrium
MRI	Magnetic Resonance Imaging
SNP	Single nucleotide polymorphism
SM	Syringomyelia
SV	Structural Variant
TPS	Total Pain Score
TSS	Total Scratch Score
WGS	Whole Genome Sequencing

Supplementary Information

The online version contains supplementary material available at https://doi.org/10.1186/s12917-025-04754-4.

Supplementary Material 1

Supplementary Material 2

Acknowledgements

The authors would like to thank the Cavalier King Charles owners and breeders for involvement in our studies and commitment to our research. We acknowledge Jennifer Massey for MRI acquisition, Brian Williams for assistance with data handling, and North Carolina State University's Neurology service for referral of dogs to our research studies.

Author contributions

CRS and NJO contributed to the planning of the study, recruitment, collection of samples, and data acquisition. JC, MWV, and KM contributed to the processing of the samples and data. CRS, MWV conducted the data analysis. ML performed sequencing. SGF and NJO reviewed the methodology. The original draft was prepared by CRS and NJO. All authors participated in the final editing and reviewing process of the manuscript.

Funding

This study was funded by the American Cavalier King Charles Spaniel Club Charitable Trust through the American Kennel Club Canine Health Foundation (Grant number 02162-MOU). Dr Sparks was funded by the National Institute of Health (Grant number F30OD025357).

Data availability

Data are available in the manuscript in the form of Tables 1, 2, 3, 4, 5 and 6; Figs. 1, 2 and 3. SNP data are available on reasonable request. WGS data are available from NCBI's SRA under BioProject PRJNA1217832.

Declarations

Ethics approval and consent to participate

All owners reviewed an informed consent form, were given the opportunity to ask questions and signed the form. All procedures were approved by NCSU's Institutional Animal Care and Use Committee (Protocol #15-003-O)."

Consent for publication

Not applicable.

Competing interests

The authors declare no competing interests.

Received: 31 January 2025 / Accepted: 14 April 2025
Published online: 03 May 2025

References

1. Hechler AC, Moore SA. Understanding and treating Chiari-like malformation and Syringomyelia in dogs. Top Comp Anim Med. 2018;33(1):1–11.
2. Sparks CR, Cerda-Gonzalez S, Griffith EH, Lascelles BDX, Olby NJ. Questionnaire-based analysis of Owner-reported scratching and pain signs in Cavalier King Charles spaniels screened for Chiari-like malformation and Syringomyelia. J Vet Intern Med. 2018;32(1):331–9.
3. Rutherford L, Wessmann A, Rusbridge C, McGonnell IM, Abeyesinghe S, Burn C, et al. Questionnaire-based behaviour analysis of Cavalier King Charles

spaniels with neuropathic pain due to Chiari-like malformation and Syringomyelia. T Vet J. 2012;194(3):294–8.
4. Cerda-Gonzalez S, Olby NJ, Griffith EH. Longitudinal study of the relationship among craniocervical morphology, clinical progression, and Syringomyelia in a cohort of Cavalier King Charles spaniels. J Vet Intern Med. 2016;30(4):1090–8. https://doi.org/10.1111/jvim.14362.
5. Ives EJ, Doyle L, Holmes M, Williams TL, Vanhaesebrouck AE. Association between the findings on magnetic resonance imaging screening for Syringomyelia in asymptomatic Cavalier King Charles spaniels and observation of clinical signs consistent with Syringomyelia in later life. Vet J. 2015;203(1):129–30.
6. Plessas IN, Rusbridge C, Driver CJ, Chandler KE, Craig A, McGonnell IM, et al. Long-term outcome of Cavalier King Charles spaniel dogs with clinical signs associated with Chiari-like malformation and Syringomyelia. Vet Rec. 2012;171(20):501.
7. Nalborczyk ZR, McFadyen AK, Jovanovik J, Tauro A, Driver CJ, Fitzpatrick N, et al. MRI characteristics for Phantom scratching in canine Syringomyelia. BMC Vet Res. 2017;13(1):340.
8. Parker JE, Knowler SP, Rusbridge C, Noorman E, Jeffery ND. Prevalence of asymptomatic Syringomyelia in Cavalier King Charles spaniels. Vet Rec. 2011;168(25):667.
9. Cerda-Gonzalez S, Olby NJ, Broadstone R, McCullough S, Osborne JA. Characteristics of cerebrospinal fluid flow in Cavalier King Charles spaniels analyzed using phase velocity cine magnetic resonance imaging. Vet Radiol US. 2009;50(5):467–76.
10. Driver CJ, Volk HA, Rusbridge C, Van Ham LM. An update on the pathogenesis of Syringomyelia secondary to Chiari-like malformations in dogs. Vet J. 2013;198(3):551–9.
11. Fenn J, Schmidt MJ, Simpson H, Driver CJ, Volk HA. Venous sinus volume in the caudal cranial fossa in Cavalier King Charles spaniels with Syringomyelia. Vet J. 2013;197(3):896–7.
12. Driver CJ, Rusbridge C, Cross HR, McGonnell I, Volk HA. Relationship of brain parenchyma within the caudal cranial fossa and ventricle size to Syringomyelia in Cavalier King Charles spaniels. J Small Anim Pract. 2010;51(7):382–6.
13. Rusbridge C, Greitz D, Iskandar BJ, Syringomyelia. Current concepts in pathogenesis, diagnosis, and treatment. J Vet Intern Med. 2006;20(3):469–79.
14. Rusbridge C, McFadyen AK, Knower SP. Behavioral and clinical signs of Chiari-like malformation-associated pain and Syringomyelia in Cavalier King Charles spaniels. J Vet Intern Med 2019;0(0).
15. Lewis T, Rusbridge C, Knowler P, Blott S, Woolliams JA. Heritability of Syringomyelia in Cavalier King Charles spaniels. Vet J. 2010;183(3):345–7.
16. Rusbridge C, Knowler SP. Inheritance of occipital bone hypoplasia (Chiari type I Malformation) in Cavalier King Charles spaniels. J Vet Intern Med. 2004;18(5):673–8.
17. Rusbridge C, Knowler SP. Hereditary aspects of occipital bone hypoplasia and Syringomyelia (Chiari type I malformation) in Cavalier King Charles spaniels. Vet Rec. 2003;153(4):107–12.
18. Cappello R, Rusbridge C. Report from the Chiari-Like malformation and Syringomyelia working group round table. Vet Surg. 2007;36(5):509–12.
19. Knowler SP, McFadyen AK, Rusbridge C. Effectiveness of breeding guidelines for reducing the prevalence of Syringomyelia. Vet Rec 2011;169.
20. Wijnrocx K, Van Bruggen LWL, Eggelmeijer W, Noorman E, Jacques A, Buys N, et al. Twelve years of chiari-like malformation and Syringomyelia scanning in Cavalier King Charles spaniels in the Netherlands: towards a more precise phenotype. PLoS ONE. 2017;12(9):e0184893.
21. Karlsson EK, Lindblad-Toh K. Leader of the pack: gene mapping in dogs and other model organisms. Nat Rev Gen 2008 -09;9(9):713–25.
22. Schoenebeck JJ, Hutchinson SA, Byers A, Beale HC, Carrington B, Faden DL, et al. Variation of BMP3 contributes to dog breed skull diversity. PLoS Genet. 2012;8(8):e1002849.
23. Ancot F, Lemay P, Knowler SP, Kennedy K, Griffiths S, Cherubini GB, et al. A genome-wide association study identifies candidate loci associated to Syringomyelia secondary to Chiari-like malformation in Cavalier King Charles spaniels. BMC Genet. 2018;19(1):16.
24. Lemay P, Knowler SP, Bouasker S, Nédélec Y, Platt S, Freeman C, et al. Quantitative trait loci (QTL) study identifies novel genomic regions associated to Chiari-Like malformation in griffon bruxellois dogs. PLoS ONE. 2014;9(4):e89816.
25. Loderstedt S, Benigni L, Chandler K, Cardwell JM, Rusbridge C, Lamb CR, et al. Distribution of Syringomyelia along the entire spinal cord in clinically affected Cavalier King Charles spaniels. Vet J. 2011;190(3):359–63.
26. Couturier J, Rault D, Cauzinille L. Chiari-like malformation and Syringomyelia in normal Cavalier King Charles spaniels: a multiple diagnostic imaging approach. J Small Anim Pract. 2008;49(9):438–43.
27. Thøfner MS, Stougaard CL, Westrup U, Madry AA, Knudsen CS, Berg H, et al. Prevalence and heritability of symptomatic Syringomyelia in Cavalier King Charles spaniels and Long-term outcome in symptomatic and asymptomatic littermates. J Vet Intern Med. 2015;29(1):243–50.
28. Peng G, Han M, Du Y, Lin A, Yu L, Zhang Y, et al. SIP30 is regulated by ERK in peripheral nerve Injury-induced neuropathic pain. J Biol Chem. 2009;284(44):30138–47.
29. Han M, Xiao X, Yang Y, Huang RY, Cao H, Zhao ZQ, et al. SIP30 is required for neuropathic pain-evoked aversion in rats. J Neurosci. 2014;34(2):346–55.
30. Zhang YQ, Guo N, Peng G, Wang X, Han M, Raincrow J, et al. Role of SIP30 in the development and maintenance of peripheral nerve injury-induced neuropathic pain. Pain. 2009;146(1–2):130–40.
31. Varma D, Salmon ED. The KMN protein network–chief conductors of the kinetochore orchestra. J Cell Sci. 2012;125(Pt 24):5927–36.
32. Lee H, Safieddine S, Petralia RS, Wenthold RJ. Identification of a novel SNAP25 interacting protein (SIP30). J Neurochem. 2002;81(6):1338–47.
33. Zhang F, Lupski JR. Non-coding genetic variants in human disease. Hum Mol Genet. 2015;24(R1):102.
34. Nalborczyk ZR, McFadyen AK, Jovanovik J, Tauro A, Driver CJ, Fitzpatrick N, et al. MRI characteristics for Phantom scratching in canine Syringomyelia. BMC Vet Res. 2017;13(1):340–2.
35. Al Dhaheri N, Wu N, Zhao S, Wu Z, Blank RD, Zhang J, et al. KIAA1217: A novel candidate gene associated with isolated and syndromic vertebral malformations. Am J Med Genet A. 2020;182(7):1664–72.
36. Seddik R, Jungblut SP, Silander OK, Rajalu M, Fritzius T, Besseyrias V, et al. Opposite effects of KCTD subunit domains on GABAB Receptor-mediated desensitization. J Biol Chem. 2012;287(47):39869–77.
37. Turecek R, Schwenk J, Fritzius T, Ivankova K, Zolles G, Adelfinger L, et al. Auxiliary GABAB receptor subunits uncouple G protein Bγ subunits from effector channels to induce desensitization. Neuron. 2014;82(5):1032–44.
38. Schwenk J, Metz M, Zolles G, Turecek R, Fritzius T, Bildl W, et al. Native GABA(B) receptors are heteromultimers with a family of auxiliary subunits. Nature. 2010;465(7295):231–5.
39. Metz M, Gassmann M, Fakler B, Schaeren-Wiemers N, Bettler B. Distribution of the auxiliary GABAB receptor subunits KCTD8, 12, 12b, and 16 in the mouse brain. J Comp Neurol. 2011;519(8):1435–54.
40. Paus T, Bernard M, Chakravarty MM, Davey Smith G, Gillis J, Lourdusamy A, et al. KCTD8 gene and brain growth in adverse intrauterine environment: A Genome-wide association study. Cereb Cortex. 2011;22(11):2634–42.
41. Zhou X, Stephens M. Genome-wide efficient mixed model analysis for association studies. Nat Genet. 2012;44:821–4.
42. Friedenberg SG, Meurs KM, Mackay TFC. Evaluation of artificial selection in standard poodles using whole-genome sequencing. Mamm Genome. 2016;27(11–12):599–609.
43. Layer RM, Chiang C, Quinlan AR, Hall IM. LUMPY: A probabilistic framework for structural variant discovery. Genome Biol. 2014;15(6).
44. Larson DE, Abel HJ, Chiang C, Badve A, Das I, Eldred JM, et al. Svtools: population-scale analysis of structural variation. Bioinformatics. 2019;35:4782–7.
45. Chiang C, Layer RM, Faust GG, Lindberg MR, Rose DB, Garrison EP, et al. SpeedSeq: ultra-fast personal genome analysis and interpretation. Nat Methods. 2015;12:966–8.
46. Pedersen BS, Quinlan AR. Duphold: scalable, depth-based annotation and curation of high-confidence structural variant calls. GigaScience. 2019;8:giz040.
47. Li H. Minimap2: pairwise alignment for nucleotide sequences. Bioinformatics. 2018;34:3094–100.

Publisher's note